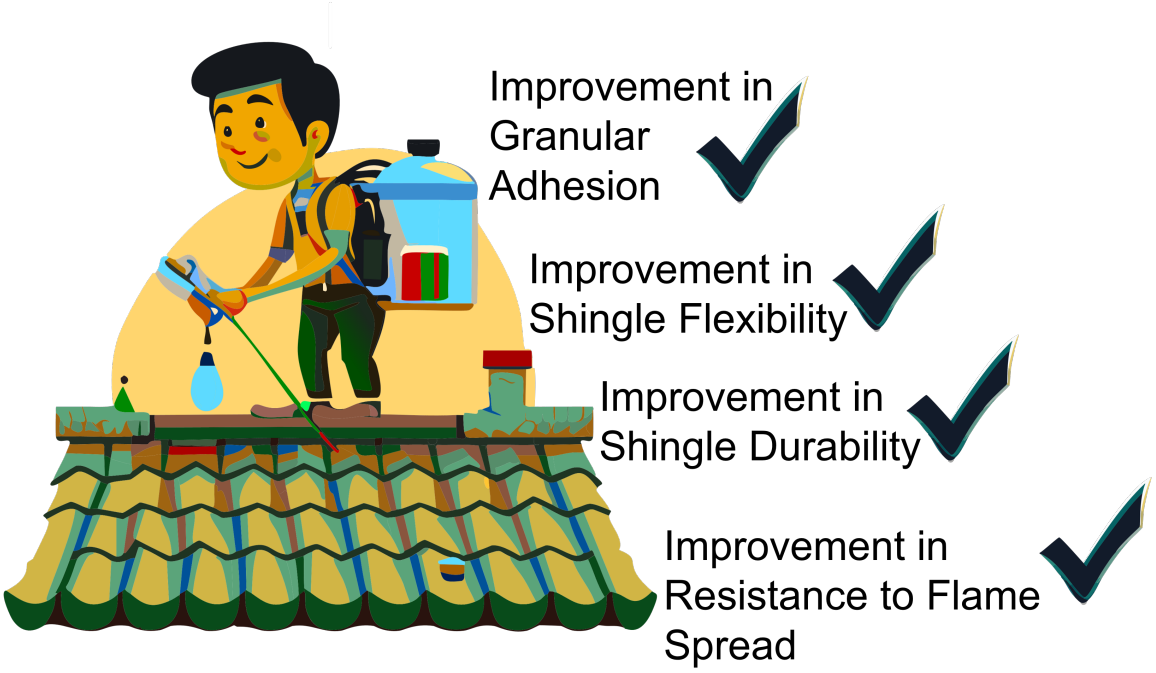
Graphical Abstract

Restoring Asphalt Shingle Integrity with Soybean Oil-Based Emulsions: A Case Study on Performance, Durability, and Sustainability

Baker W. Kuehl, Andrew Becker, Sharan Raman, Anna McCaslin, Jefferson Roberts-Dobie, Michael Forrester, Nacu Hernandez, Austin Hohmann, R. Chris Williams, Eric W. Cochran



Abstract image of a contractor applying a soybean-derived reactive rejuvenator emulsion and its benefits to asphalt shingle rejuvenation.

Restoring Asphalt Shingle Integrity with Soybean Oil-Based Emulsions: A Case Study on Performance, Durability, and Sustainability

Baker W. Kuehl*, Andrew Becker*, Sharan Raman, Anna McCaslin, Jefferson Roberts-Dobie, Michael Forrester, Nacu Hernandez, Austin Hohmann, R. Chris Williams, Eric W. Cochran[a,**]

[a]*Department of Chemical & Biological Engineering, Iowa State University, Ames, Iowa 50011, United States*

Abstract

Here we report the revitalization of aged asphalt roofing shingles by applying semi-epoxidized soybean oil (SESO) as an aqueous emulsion. We hypothesized that the reactivity of SESO oxirane with oxidized components of the shingle asphalt composition would improve durable performance through an internal plasticization mechanism. Using SESO emulsions at 10 wt% and 30 wt%, together with a 10 wt% soy-based methyl ester emulsion (SME) as an inert control, we applied 200 mL/m² to 3-tab and architectural shingles in both new and 15+ year-aged states. Key performance metrics were grit adhesion, flexibility, crack, hail, and flame resistance. Although all treatments improved grit retention, both SESO-based emulsions significantly outperformed SME treatment in all other respects. All treatments reduced the flexural modulus due to plasticization; Aged samples treated with 10 wt% SESO and SME exhibited values comparable to new shingles. Although 30 wt% SESO-treated samples were overly softened, the 10 wt%-treated shingles exhibited restored ductility, hail resistance, and reduced flame spread compared to both SME-treated and untreated specimens. The results suggest that SESO is effective in penetrating and reacting with asphalt in aged shingles, restoring many key aspects of shingle performance to those of new shingles. This strategy could support the circular economy by extending the service life of asphalt shingles.

Keywords: shingles, asphalt, roofing, soybean oil, asphaltenes

*Contributed equally to this work.

**Corresponding author.

Email address: ecochran@iastate.edu (Eric W. Cochran)

1. Introduction

Asphalt shingles are the roofing material of choice for more than 80% of U.S. residential homes [1] and cover 27% of U.S. commercial buildings [2]. The provision of new and replacement shingles is quite resource-intensive; in 2014, for example, the U.S. asphalt shingle and coating materials industry 2014 consumed approximately 730 million kWh of electricity and 10 billion cubic feet of natural gas [3]. In 2021, roof manufacturers in the US and Canada shipped approximately 1.7 billion square metres (183 million roofing squares) of roofing shingles [4], as illustrated in Figure 1. Given the weight range of 200–300 pounds per "square" [5], this volume of shipment translates to an estimated 17–25 million metric tons of shingles consumed each year, generating approximately 10 million tons of waste from end-of-life shingles or tear-offs. [6, 7] The diversion of this waste from landfills is of paramount importance, with many jurisdictions having placed blanket bans on landfill disposal due to concerns about toxic runoff. Although shingle manufacturers continue improving the use of recycled shingle content in new shingles, recycling rates remain below 5%. Most tear-off shingles are *down-cycled*, in which shingle recycling facilities grind them for various purposes such as ground cover, dust control, or as a mix design component in asphalt pavement. Recycled asphalt shingles (RAS) are frequently used in the asphalt pavement industry, alongside recycled asphalt pavement (RAP). [8–10] However, using RAS on pavements is more challenging than RAP due to the extremely stiff formulations of the binder used and the composite nature of asphalt shingles, comprising only about 19-22 wt% asphalt. In addition, they consist of a fiberglass mat, providing strength, which accounts for 2-15 wt %; mineral aggregate, 20-38 wt %, which provides hail protection and texture; and mineral filler/stabilizer, constituting 8-40 wt%, crucial for ensuring durability and weather resistance. These diverse materials complicate the recycling process for RAS compared to the more homogeneous RAP, which is essentially only aggregate and asphalt. Although RAS can be used on asphalt pavements as a component of the aggregate phase, rarely exceeding 5 wt %, its properties are unpredictable and deteriorate the pavement quality. Some jurisdictions are quite sensitive to using their pavement infrastructure as landfills and accordingly disallow RAS use. Consequently, there is a growing desire to enhance the longevity of asphalt shingles to prevent them from ending up in landfills or being used in asphalt mix designs. By improving the durability and lifespan of asphalt shingles, the frequency of their replacement on roofs can be reduced, thereby minimizing the environmental impact and the burden on shingle stockpiles. [11, 12] While this can be achieved through advances in shingle

manufacturing technology, methods to prevent or even reverse the effects of aging on existing shingles are of critical importance.

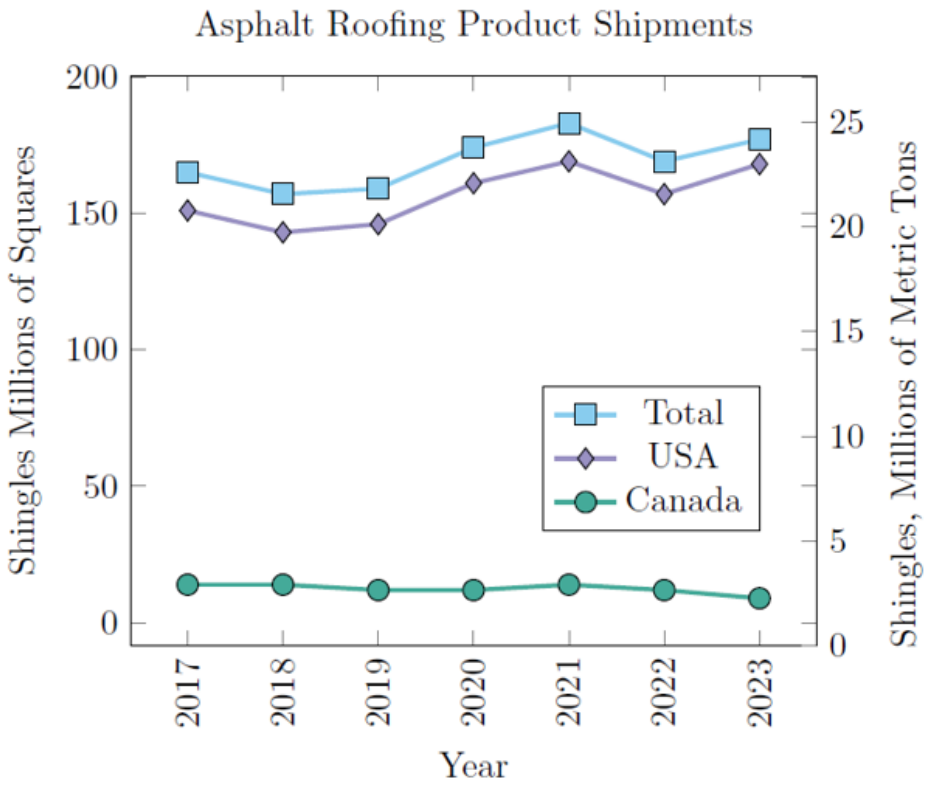


Figure 1 Amount of asphalt shingles shipped throughout North America

The development of such methods may benefit from advances in the asphalt pavement industry concerning the restoration of aged pavements. Recently, there has been a notable increase in the use of recycling aids known as rejuvenators in processing RAP. Rejuvenators are additives designed to restore the original properties of the aged asphalt binder in RAP, effectively improving its workability and performance. These additives work by replenishing the oils and resins lost during the ageing process, thereby improving the flexibility and durability of the recycled material. The introduction of rejuvenators has significantly improved the quality and usability of RAP, allowing higher percentages of recycled content in new asphalt mixtures without compromising performance. [13–15]

Although many rejuvenators have shown the ability to improve the workability of aged asphalt, most do not do anything at the molecular level to address oxidative damage. Chemically inert additives, especially those chemically different from asphalt, merely adjust viscosity, albeit temporarily, with embrittlement occurring as the additive leaches out over time. Hohmann et al. introduced a new class

of *chemically reactive* rejuvenators, which possess reactive chemical moieties capable of rebalancing the saturates, aromatics, resins, and asphaltenes (SARA) network, thereby reversing the aging of the asphalt binder. [16–19] These advanced materials are engineered with specific chemical functionalities that allow them to interact more profoundly with the asphalt's molecular structure. [20, 21] Reactive rejuvenators covalently bond to the agglomerated asphaltenes within the asphalt mix, repeptizing the large asphaltene structures that cause brittleness and reintegrating them into the binder. cite elkashefInvestigationFatigueThermal2018,linEffectRejuvenatorSealer2013,sotoodeh-niaEffectTwoNovel2019 This restoration is crucial for reversing the material's brittleness and reducing its susceptibility to cracking. By restoring the chemical composition of aged asphalt, these reactive rejuvenators facilitate a higher proportion of RAP in new installations, improving sustainability and resource efficiency in the asphalt industry. [22–24]

Similar to the deterioration of RAP, asphalt roofing materials are also subject to ageing and environmental wear. [25, 26] The degradation of these materials, attributed to UV exposure, thermal variations, and oxidative ageing, leads to loss of volatiles and consequently increased brittleness, decreased pliability, and compromised adhesive characteristics that are essential for the granular coating's durability and the bond of the lower lip of each shingle to the adhesion strip of the shingle beneath them. [27–29] The ageing-related rigidity and propensity to crack in RAP and RAS are paralleled in aged roofing materials, heightening susceptibility to damage from hail, wind, and ice. These overlapping degradation phenomena accentuate the need for rejuvenation interventions, which can improve and restore the original qualities of asphalt substrates. [30–38] Recent advancements in asphalt modification emphasize sustainable solutions that combine laboratory performance with field applicability. For example, Jin et al. demonstrated that overlays incorporating recycled rubber and tire fabric fibers improve durability and crack resistance in controlled and in-use environments. Similar work has extended to stress-absorbing membrane interlayers using rubber-modified binders, effectively mitigating reflective cracking during resurfacing. Additionally, integrating tire-derived aggregate in the subgrade has been shown to enhance the long-term performance of rubber-modified asphalt mixtures under aging and load. These studies underscore the potential of reactive and recycled materials in restoring aged infrastructure. [39–41] Building on this momentum, our work explores the reactivity of SESO—a multi-epoxy functional oil—with degraded asphalt shingles, aiming to demonstrate not just surface-level improvement, but chemical-level restoration of aged binder performance.

In this work, we develop and apply a new reactive emulsion made from semi-epoxidized soybean oil (SESO), specifically formulated to rejuvenate asphalt roofs, using the exact asphaltene stabilization mechanism illustrated by Hohmann et al. in RAP restoration. [19] We hypothesized that the reactivity of SESO would promote long-lasting restoration of the properties of the shingles due to covalent bonding; for comparison, we also formulated an inert treatment emulsion from soy methyl esters (SME). This innovative approach focuses on the chemical remediation of aged asphalt shingles to enhance their durability, flexibility, and grit adhesion. As shingles age, they become brittle and lose their protective granules, leading to accelerated degradation and a reduced lifespan. The reactive emulsion described here is designed to penetrate the old shingles deeply, restore essential oils lost over time, and effectively bond the surface granules. By improving these key properties, such treatments could extend the functional life of the shingles, reduce waste from roof replacements, and offer a much more environmentally friendly alternative to a complete roof overhaul. We examine the formulation's efficacy, application methods, and long-term benefits for residential roofing systems through comprehensive laboratory tests.

2. Experimental Methods

2.1. Materials

Semi-Epoxidized Soybean Oil (SESO) with 2.5 wt% oxirane content and Soy Methyl Ester (SME, soy-based biodiesel) were generously supplied by CHS, Inc. (Mankato, MN) and were used as received. Soybean lecithin was obtained from Croda International and also utilized as received. The aqueous phase for the emulsions was prepared using city water, and xanthan gum was sourced from Walmart. Chemical structures appear in Figure S1.

2.2. Formulation of Emulsions

Emulsions were prepared by adding 10 g of lecithin to 250 g of oil, SESO, or SME, and blending with a mechanical agitator. The oil phase was then combined with 750 g of city water and 0.7 g of xanthan gum and mixed for 5 minutes with an overhead stirrer to form a pre-emulsion. The pre-emulsion was processed with an IKA high-shear immersion lab mixer to achieve the final emulsified product.

2.3. Shingles

New Owens Corning Supreme 3-tab shingles and Atlas Castlebrook architectural shingles were purchased from Menards. Aged 3-tab and architectural shingles were taken from two roofs in central Iowa, 42°N, 94°W, that had been in place for 15+ years. Only the sun-exposed, lower portion of the shingle was tested for these aged samples. Shingles were evaluated in untreated and treated states. Treated shingles were sprayed with 200 sq. ft/gallon (200 mL/m^2) of SESO/emulsion via a High Volume Low Pressure (HVLP) sprayer. The shingles were then placed in a 60 °C oven for 48 hours to allow the SESO to permeate the material. This treatment simulates exposure to summer rooftop temperatures. [42]

2.4. 3pt Bend Testing

The shingle samples were sliced into five two-inch-wide strips and tested in a 3-point bend configuration with a 1 cm diameter cylindrical contact surface using an Instron load frame. The shingles were loaded with the bottom points of contact spaced 30 mm apart and the grit side facing upward so that cracks would form on the underside of the shingle and were tested at a temperature of 21°C (70°F), with a 1 mm/second loading rate.

2.5. Grit loss Testing

An aged 3-tab shingle was tested according to ASTM D4977 Standard Test Method for Granule Adhesion to Mineral Surfaced Roofing by Abrasion samples. The ASTM test measures grit loss on two 50.8 mm $\times$ 229 mm (2 in. $\times$ 9 in.) samples with a 2268 $\pm$ 7 g load (5 lb) load on 880 bristles made of 0.305 mm (0.012 in.) diameter tempered steel wire.

The ASTM D4977 grit loss test resulted in a 10% mass loss for the tested portion of the untreated sample. We developed a less aggressive method that provided conditions similar to the abrasion caused by wind and snow. We tested a larger area than the ASTM test for better statistical repeatability. Four 30.5 cm $\times$ 15 cm (12 inch $\times$ 6 inch) samples were cut from the lower, sun-exposed half of each new, aged, 3-tab and architectural shingle. After labelling and weighing, the shingles were placed on the floor randomly. A Dirt Devil ProPower carpet and hardwood floor vacuum set on the lowest floor was passed forward and backward over the shingles at a speed of 0.5 m/s. After 10 forward and reverse passes, the shingles were weighed and shuffled for the subsequent 10 passes. All weights were recorded with 0.01 g sensitivity.

2.6. FTIR

Fourier transform infrared (FTIR) spectra were collected for SESO, untreated shingles, and SESO-treated shingles using a TATR Crystal FTIR. 64 scans were collected per run with a resolution of 4 cm-1 for 500 – 4000 cm-1.

2.7. ^{1}H-NMR

Molecular changes following SESO treatment were evaluated using a Bruker AVII 600 MHz 1HNMR spectrometer. Samples were dissolved in deuterated chloroform ($CDCl_3$) with tetramethylsilane (TMS) used as the internal standard unless otherwise noted. Each spectrum was acquired over 16 scans with a 1-second delay between pulses.

2.8. DSC

Differential scanning calorimetry (DSC) probed thermal transitions in untreated and SESO-treated asphalt shingles. Samples were first dried at 100 °C to remove residual moisture, then heated from –100 °C to 150 °C at a rate of 10 °C/min using a TA Instruments Discovery 2500. The resulting thermograms showed a shift in the glass transition region for the treated shingles, indicating changes in the mobility and crosslink density of the asphalt binder. These thermal shifts are consistent with covalent interaction between the SESO formulation and reactive sites in the aged asphalt, complementing the molecular evidence provided by ^{1}H-NMR.

2.9. Flame spread testing

The ASTM E108 flame testing was conducted to assess the fire resistance of treated asphalt shingles, following the standard procedures outlined for roofing materials. Specifically, the “spread of flame” test was performed, where a calibrated gas flame and air current were applied continuously to test samples mounted on inclined decks. For each test, a shingled 8’ $\times$ 3.3’ deck was placed at a 5:12 slope, and its edge was ignited with a gas torch for 10 minutes at an air velocity of 1056 ft/min, reaching a temperature of 1400 °C. The flame propagation distance was recorded, with particular attention to any sustained flaming or material displacement. Shingles treated with SESO and SME emulsions and untreated controls were subjected to this evaluation to determine their ability to resist flame spread. Recognizing the potential concern regarding flammability raised by reactive emulsion treatments, additional oxygen index tests (ASTM D2863) were considered. However, guidance from Grayson and Hirschler [43] and the scenario-based approach of Guillaume [44] indicates that flame

Table 1 Formulation of semi-epoxidized vegetable oil emulsions

Sample Code	SESO or SME (wt%)	Lecithin (wt%)	Water (wt%)	Xanthan Gum (wt%)
SME	10	1	89	0.07
10	10	1	89	0.07
30	30	1	69	0.03

spread and heat release tests provide more direct insight into real-scale fire performance. Therefore, additional oxygen index testing was deferred at this stage.

3. Results and Discussion

SESO and SME emulsions, as detailed in Table 1, were formulated to assess their compatibility and effectiveness as a function of oxirane content (0%, SME, and 2.3 wt%, SESO) and total oil loading. The emulsions are prepared with varying concentrations of oil, lecithin, water, and xanthan gum. Formulation "10" consists of 10 wt% SESO, 1 wt% lecithin, 89 wt% water, and 0.07 wt% xanthan gum. Formulation "30" contains 30 wt% SESO, with 1 wt% lecithin and 0.03 wt% xanthan gum. "SME" contains 10 wt% soy methyl ester (biodiesel) to assess the performance of an inert softening agent compared with the reactivity of the SESO emulsions. The critical feature of SESO in these emulsions that differs from conventional rejuvenator emulsions is the presence of epoxide groups, which are crucial for rejuvenating aged asphalt shingles. These reactive species covalently bond with the oxidized asphaltenes in the shingle asphalt binder. This reaction helps to reintegrate asphaltenes into the binder matrix and enhances the overall structural integrity. The binding of SESO to damaged asphaltenes is hypothesized to reverse embrittlement and ductility loss typical of aged shingles, contributing to improved durability and extending the life of the roofing material. Using lecithin and xanthan gum in the emulsion ensures that the SESO is evenly distributed and stable, allowing maximum interaction between the epoxide groups and the asphaltenes during treatment.

We applied these treatments at 200 sq ft. /gallon to new and aged 3-tab and architectural shingles. Samples are encoded as the type of treatment (Untreated, 10% SESO, 30% SESO, or 10 %SME), followed by the shingle age (New or Old), and the shingle type (3Tab or Architectural). The primary differences between 3-tab and architectural shingles are their appearance, durability, and cost. 3-tab shingles are flat and uniform in size and shape, resulting in a smooth, consistent look.

In contrast, architectural shingles, also known as dimensional or laminated shingles, have a layered and textured appearance mimicking the look of natural wood or slate, offering more visual depth. Regarding durability, 3-tab shingles are thinner and typically have a lifespan of around 20–25 years, while architectural shingles are thicker, more durable, and can last between 30–50 years, with better resistance to wind and impact damage. Concerning cost, 3-tab shingles are less expensive due to their more straightforward design and lower material usage. In contrast, architectural shingles are more costly due to their enhanced durability and aesthetic appeal. Generally, 3-tab shingles provide an essential and affordable option, while architectural shingles offer a longer-lasting, visually striking alternative.

Flexural stress-strain data from 3-point bend tests appear in Fig 2 and Table S1. The higher quality of architectural shingles is evidenced by stiffness and strength values slightly higher than those of the 3-tab samples; however, as these shingles age, the effects of embrittlement become far more pronounced with nearly 300% increases for architectural shingles compared to roughly 200% increases in 3-tabs. Notably, flexural strain results indicate a significant increase in flexibility, especially in older shingles treated with 30 wt% SESO (30-O-3T), achieving the highest strain at 10.0 ± 1.2 MPa. This increased tolerance to bending underscores that SESO markedly improves the ductility of aged, previously brittle shingles, enhancing their capacity to accommodate structural movements without cracking. While the SESO treatment indeed lowers the maximum stress values, as seen in older shingles treated with 30 wt% SESO (30-O-A), which displayed a reduced stress capacity of 2.8 ±0.4 MPa compared to untreated new architectural shingles (U-N-A) at 16.6 ±1.8 MPa, this reduction should be viewed positively. The decrease in maximum stress levels corroborates the softening effect of the SESO treatment, affirming its role in rejuvenating the asphalt binder within the shingles.

This softening is further evidenced by the flexural modulus data, which appears in Fig. 3, where a substantial reduction in stiffness in SESO-treated shingles (30-O-3T showing a modulus of 2.9 ± 0.4 MPa) compared to untreated counterparts, highlights the success of SESO in restoring flexibility. This restored flexibility is advantageous for the thermal and physical adaptation of the shingles, enhancing their overall functionality. The results collectively suggest that SESO treatments rejuvenate aged shingles and contribute positively to their long-term performance by enabling them to better withstand environmental stresses without compromising their integrity.

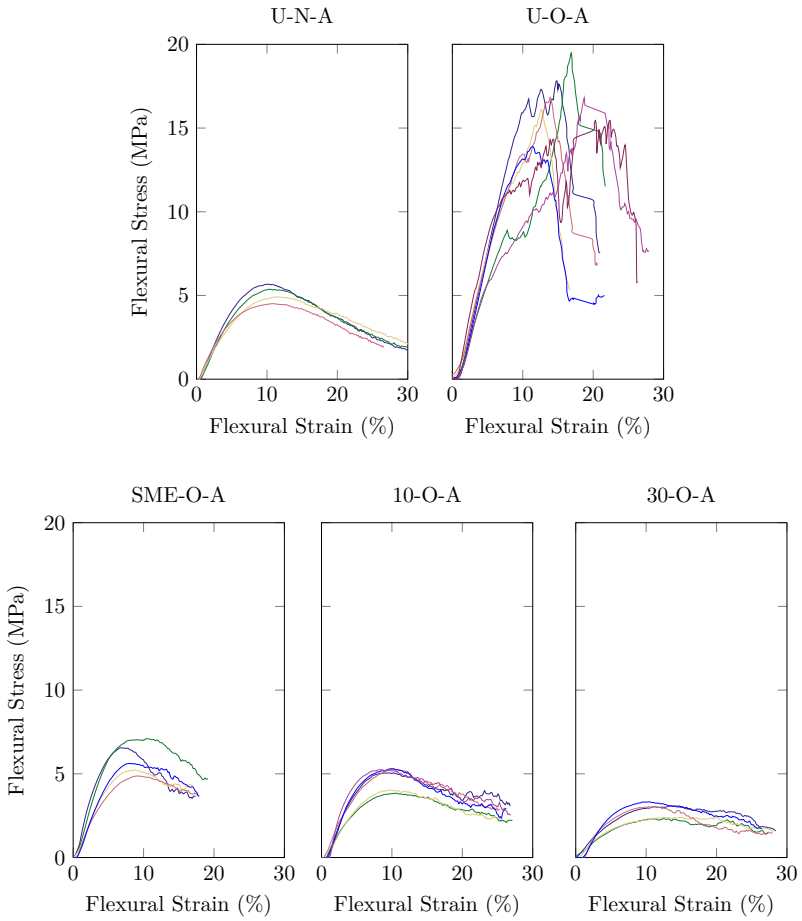


Figure 2 3 point bend test results for 3-tab (left) and architectural (right) shingles. The top row shows the strength (maximum flexural stress), while the bottom row shows the shingle stiffness (flexural modulus). 10 wt% SESO emulsions restore the flexibility of old brittle shingles (10-O-A) to near that of new shingles (N-Untreated). The jagged discontinuities in the plots of the old shingles are where small or large cracks occurred in the shingles.

While architectural shingles exhibit slightly higher stiffness and strength values than 3-tab samples, indicating their superior quality, they also experience more pronounced effects of embrittlement with ageing. Specifically, architectural shingles show nearly 300% increases in stiffness and strength due to ageing, compared to roughly 200% increases in 3-tab shingles. This embrittlement leads to reduced flexibility and increased susceptibility to cracking. Notably, the flexural strain results indicate a significant increase in flexibility in aged shingles treated with 30 wt% SESO (30-O-3T), achieving the highest strain at $10.0 \pm 1.2\%$. This result underscores that SESO markedly improves the ductility of aged, previously brittle shingles, enhancing their capacity to accommodate structural movements without cracking. This effect is beneficial while the SESO treatment lowers the maximum stress values.

For example, aged shingles treated with 30 wt% SESO (30-O-A) displayed a reduced stress capacity of 2.8 ± 0.4 MPa compared to untreated new architectural shingles (U-N-A) at 16.6 ± 1.8 MPa. The decrease in maximum stress levels corroborates the softening effect of the SESO treatment, affirming its role in rejuvenating the asphalt binder within the shingles. This softening effect is further validated by the flexural modulus data, where a substantial reduction in stiffness in SESO-treated shingles (e.g., 30-O-3T showing a modulus of 2.9 ± 0.4 MPa) compared to untreated counterparts highlights the success of SESO in restoring flexibility. This restored flexibility is advantageous for the thermal and physical adaptation of the shingles, enhancing their overall functionality. These results suggest that

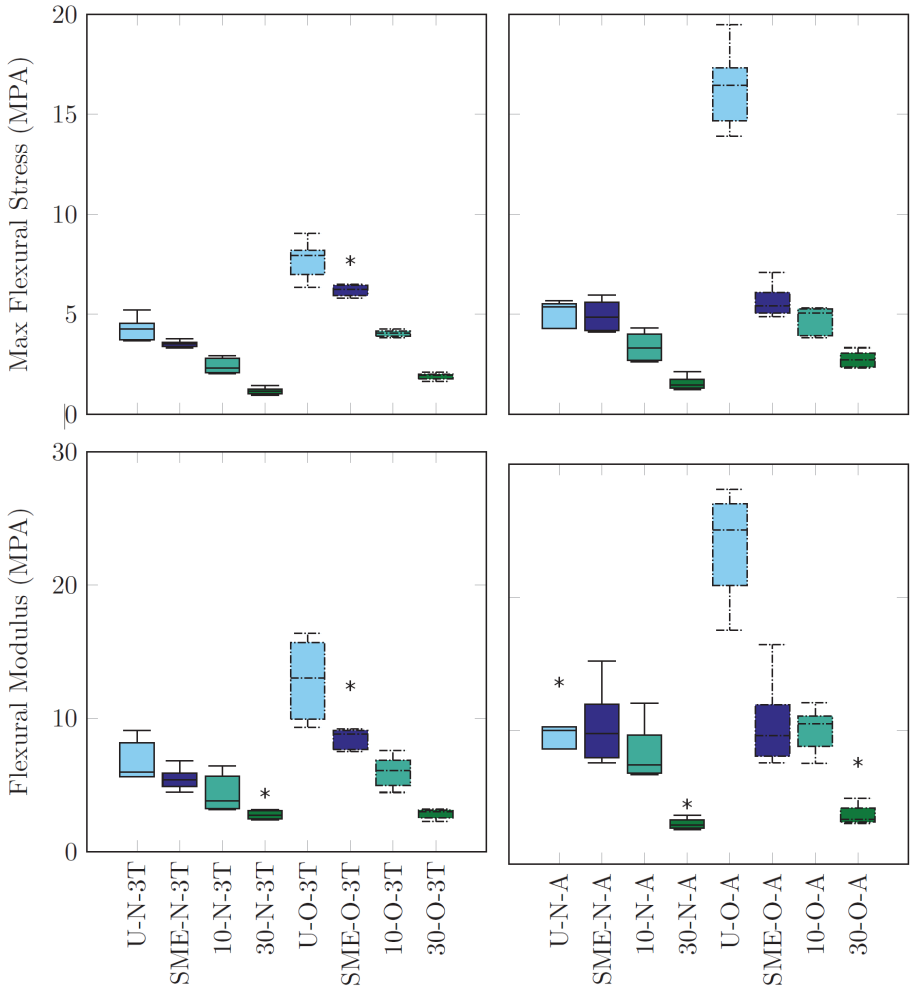


Figure 3 Box and whisker plots showing maximum flexural stress (top) and flexural modulus (bottom) across treated and untreated shingles under different conditions: unweathered (U), SME-aged (SME), and oven-aged (O), each tested in either the 3-tab (3T) or architectural (A) format. SESO treatments at 10 wt% and 30 wt% levels are compared against controls.

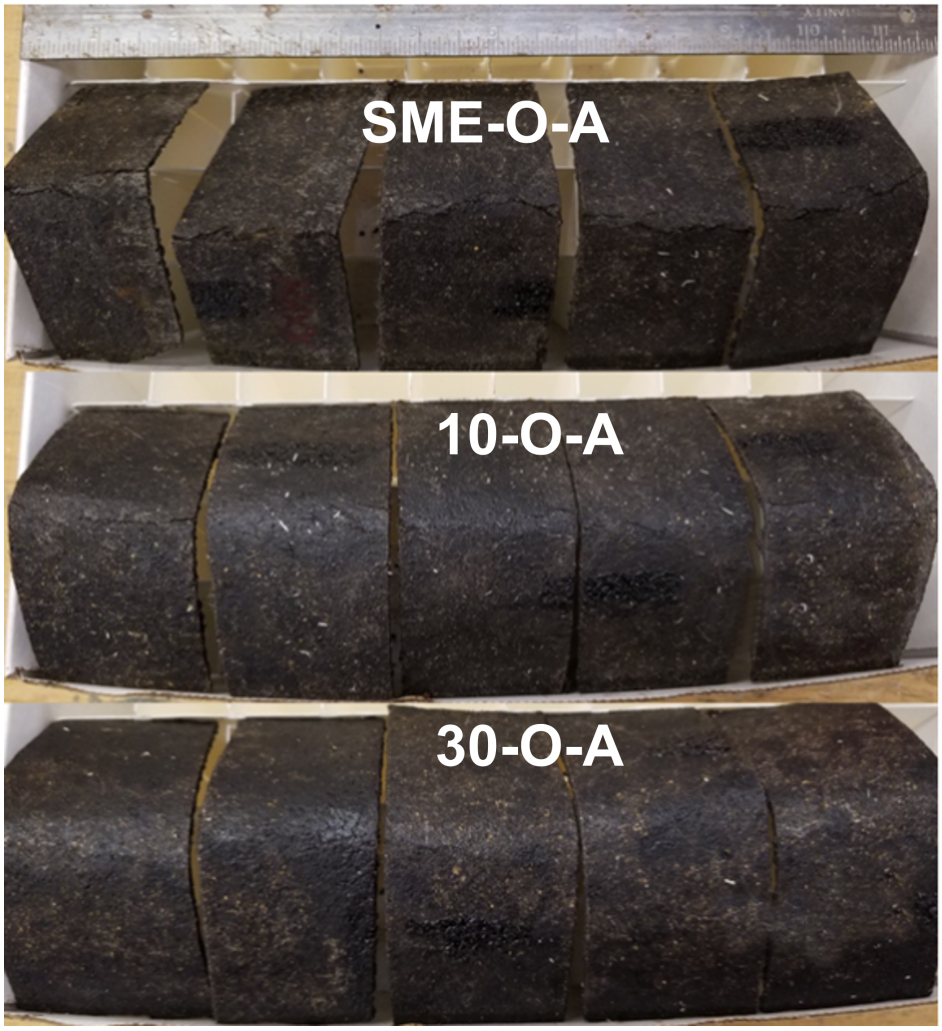


Figure 4 Visual comparison of flexural cracking behavior in oven-aged architectural shingles. Samples include SME-treated (SME-O-A), 10 wt% SESO-treated (10-O-A), and 30 wt% SESO-treated (30-O-A) shingles. The SME-O-A sample shows pronounced transverse cracking and visible edge damage. In contrast, SESO-treated samples display reduced crack formation and improved edge integrity, with the 30 wt% treatment exhibiting the least visible damage.

SESO treatments rejuvenate aged shingles and contribute positively to their long-term performance by enabling them to better withstand environmental stresses without compromising their integrity.

Visual inspection of asphalt shingles after surface treatment and bending, as shown in Figure 4, reveals significant differences in performance. A comparative analysis of shingle treatments shows that the SME-treated shingles exhibit visible surface cracks, highlighting a stark contrast in performance. These cracks indicate a failure to restore or maintain the shingle's original pliability, potentially compromising its integrity and leaving it vulnerable to further damage and degradation. The presence

of such cracks is a clear indicator that the SME fails to reinforce the asphalt matrix against the stresses experienced during the bending test. This deficiency could lead to accelerated deterioration when the shingles are exposed to real-world environmental conditions, such as temperature fluctuations and physical impacts. Beyond the effects on appearance, cracks diminish the shingle's protective properties and the longevity and performance of roofing systems. In contrast, shingles treated with either 10 wt% or 30 wt% SESO emulsions retained their structural integrity remarkably well, bending smoothly without visible damage, suggesting a significant restoration of the flexibility of the asphalt. The degree of flexibility enhancement is proportional to the SESO concentration.

Granules, as a principal structural component of the shingle, erode as the shingle ages. This process hastens with the embrittlement of the asphalt binder. Accordingly, effective rejuvenating treatments extend the shingle's lifetime by improving granule adhesion. The ASTM D4977 test aggressively measures this property by rapidly passing a weighted brush over the shingle surface 50 times over 60 – 70 s over a 38 mm $\times$ 152 mm region. Total mass losses are plotted in Figure 5, and range from 20.3% for SME-N-A to 7.64% for 30-N-A. However, since the aggregate comprises 20-38% of the shingle, the severity of the test hinders differentiation amongst all but 30-N-A. The gentler grit loss tests performed with a commercial floor vacuum provided a much more explicit comparison of how the emulsions changed the grit adhesion, shown in Figure 6.

In all roofing types tested, SESO treatments significantly reduced grit loss compared to untreated controls. The 30 wt% SESO formulation, in particular, consistently minimized grit loss across architectural shingles, except the weathered sample, where some loss remained evident. The consistency in results between new and old 3-tab shingles suggests that SESO's mechanism of enhancing grit adhesion is effective irrespective of the initial condition of the shingles. In contrast, the results for the architectural shingles indicated a less pronounced difference between the treatments, although the SESO formulations still improved over the untreated shingles. In particular, the old architectural shingles exhibited the highest overall grit loss. However, the application of 30 wt% SESO significantly reduced the loss of grit, highlighting its potential to restore integrity to even the most deteriorated shingles. The comparative underperformance of the SME treatments in all types and conditions of shingles suggests that the SESO formulations offer a more robust solution to enhance the longevity and durability of asphalt shingles. The observed reduction in grit loss can be attributed to the presence of epoxide rings in the SESO structure, which are chemically reactive and are capable of forming new covalent bonds with

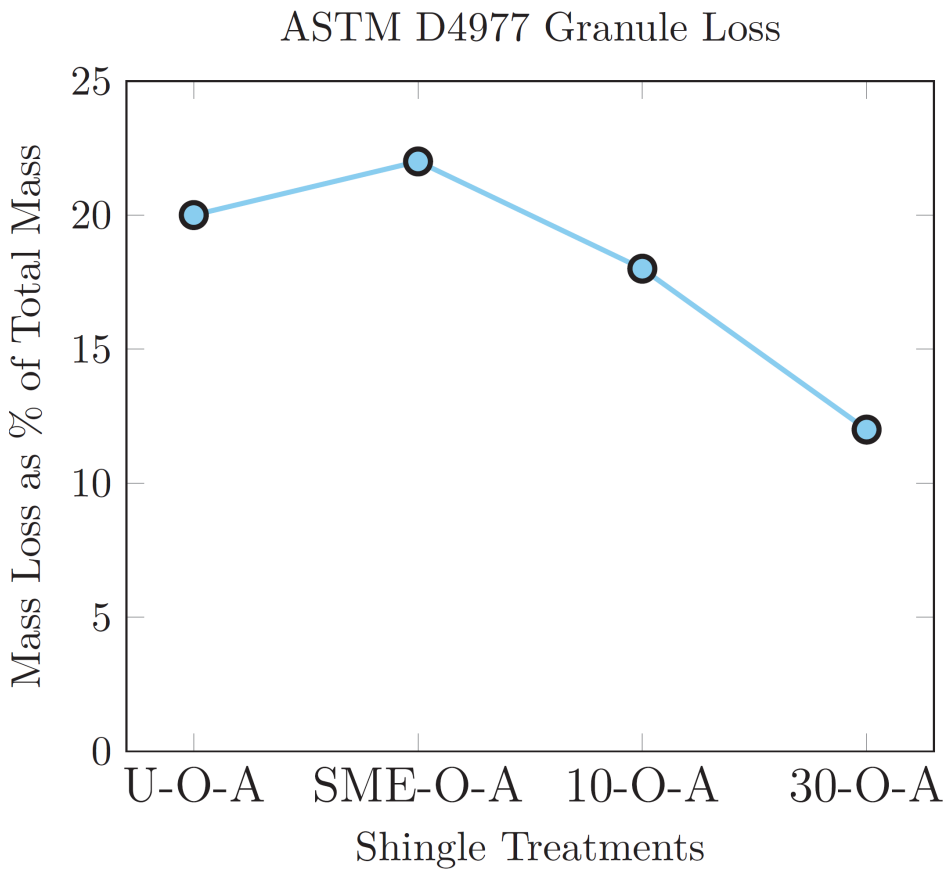


Figure 5 The graph illustrates the mass loss as a percentage of total mass for untreated shingles and shingles treated with different percentages of SME and SESO. Untreated shingles exhibit approximately 20 wt% mass loss. Shingles treated with 10 wt% SME show a slight increase in mass loss to around 22 wt%. In contrast, treatments with 10 wt% SESO and 30 wt% SESO reduce mass losses, with approximately 18% and 9%, respectively.

the asphaltenes in the asphalt binder. These new bonds contribute to a more robust binder-aggregate interaction, thereby enhancing the adhesion of the grit particles to the shingle surface. This chemical bonding strengthens the shingles' resistance to mechanical abrasion and enhances their overall structural integrity.

Figure 7 shows FTIR spectra that offer molecular-level evidence supporting the presence of chemical changes in the treated asphalt shingles. Compared to the untreated sample (U-O-A), neat SESO and 10-O-A–treated samples show distinct differences in absorbance intensity and band definition across regions associated with hydroxyl, carbonyl, and ether functionalities. These shifts and enhancements suggest new chemical environments likely arising from covalent interactions between the treatment formulations and the asphalt matrix. In particular, increased absorbance near 1700 cm^{-1} and 1100

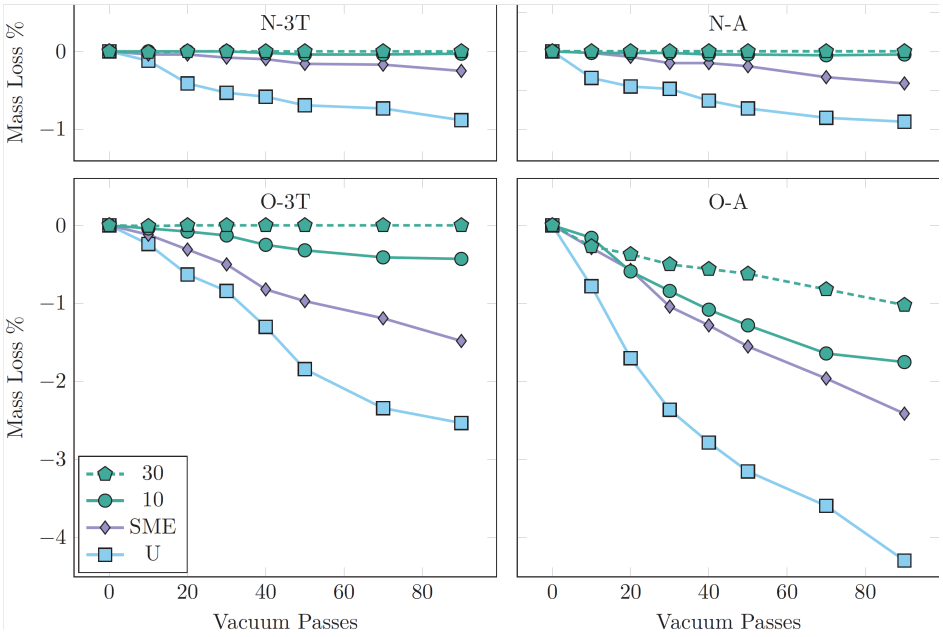


Figure 6 Grit mass loss during repeated vacuum passes for SESO-treated and untreated shingles. Panels represent normalized mass loss (in grams) across different shingle types and aging conditions: N-3T (unaged), O-3T (oven-aged), and additional configurations (right). Each curve corresponds to a treatment group: 30 wt% SESO (pentagons, dashed), 10 wt% SESO (circles), SME-aged (diamonds), and untreated (squares). SESO-treated samples retained surface granules more effectively than untreated and SME-aged shingles, with the 30wt% formulation showing the least grit loss under both unaged and aged conditions.

cm^{-1} is consistent with the introduction of carbonyl and C–O bonds, respectively. This supports the hypothesis that the treatment is not simply physical but involves chemical bonding. Further confirmation that SESO chemically reacts with the asphalt matrix, rather than merely coating or plasticizing it, we performed both ^{1}H-NMR and differential scanning calorimetry (DSC) analyses as shown in Figure 8 and Figure S2. The NMR spectra shown in Figure S2 revealed a consistent decline in the intensity of the oxirane proton signal (2.7–3.3 ppm) with increasing amounts of aged shingle material, indicating that epoxide groups were consumed during the reaction. The calculated oxirane-to-SESO proton ratio decreased from 2.34 in pure SESO to 1.18 and 0.92 in 1:1 and 1:2 SESO-to-shingle mixtures, respectively, demonstrating increasing conversion with asphalt exposure. In parallel, DSC analysis showed changes in the thermal profile of the treated shingles, including shifts in the glass transition temperature, which suggest alterations to the molecular structure of the asphalt. These combined results support the conclusion that SESO undergoes a chemical reaction likely involving covalent bonding with components of the asphalt binder.

The SESO treatment does not interfere with shingle-to-shingle adhesion during installation, owing

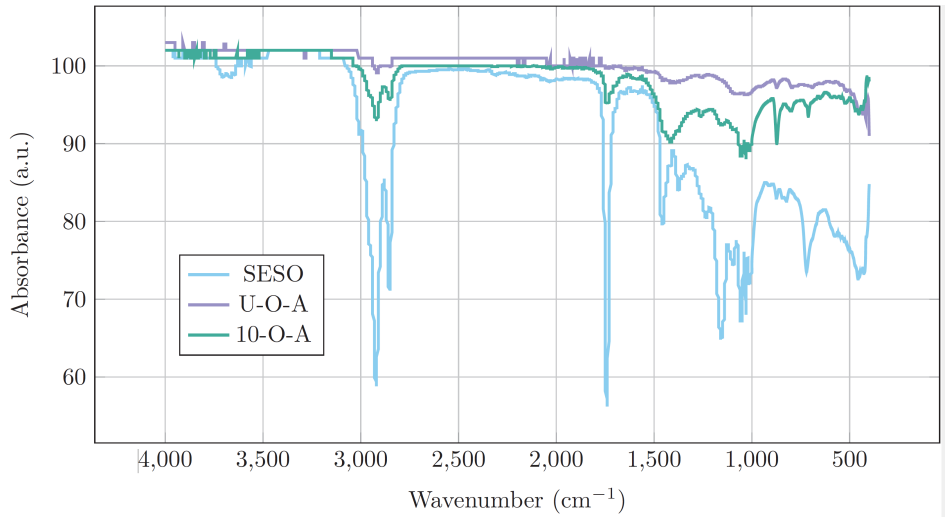


Figure 7 (FTIR) spectra comparing untreated asphalt shingles (U-O-A), shingles treated with the SESO formulation, and those treated with the 10-O-A formulation. The plot highlights characteristic absorbance features across the fingerprint region (4000–500 cm^{-1}), revealing changes in functional group presence and intensity following treatment.

to its application method and physical properties. The coating is applied exclusively to the upper, granule-covered surface of the shingle, well away from the adhesive sealant strip on the underside. Once cured, the SESO layer remains fixed and does not migrate under typical storage or roof-deck temperatures. It does not soften or create a barrier that would impede bonding. Because it leaves the adhesive interface untouched and does not alter surface energy at the contact zone, treated shingles maintain usual tack and seal when installed, as confirmed in mock installation trials.

Regarding environmental exposure, while leaching tests were not part of this study, the SESO formulation is designed to bond and crosslink with the asphalt surface during application chemically. This chemical integration creates a stable, water-insoluble layer unlikely to wash off during rainfall. Since the coating integrates with the shingle rather than existing as a loosely bound film, the likelihood of rainfall-induced loss is expected to be low. Further weathering studies would be valuable to confirm long-term durability, but the formulation's reactive chemistry supports a low leaching risk under typical conditions.

Figure 9 denotes the results of resistance to simulated hail damage, a risk with significant implications for the roof's longevity. The experiment employs a paintball gun to simulate the kinetic force of hailstones, an approach that seeks to replicate the punctual stress typically inflicted during hail events. Two samples are shown: untreated shingles (U-O-A), which exhibit extensive damage characterised

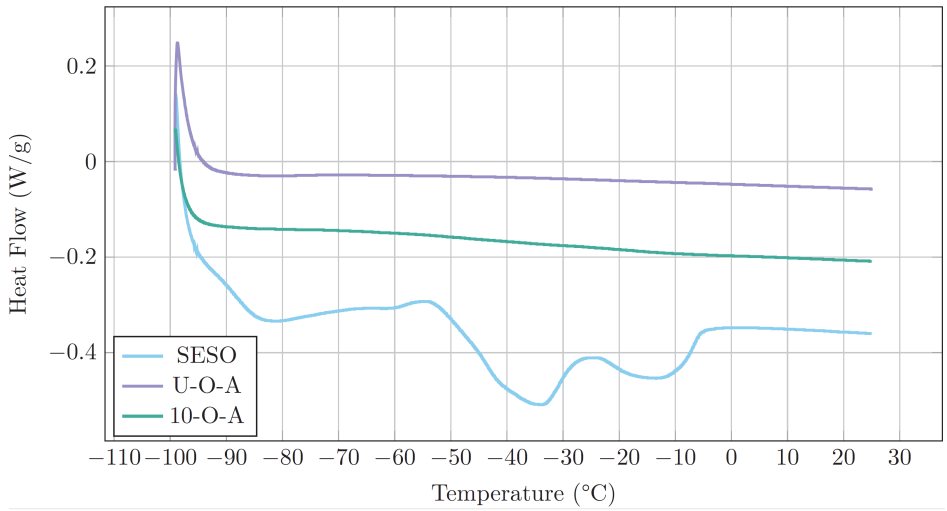


Figure 8 DSC curves of untreated shingles (U-O-A), and those treated with SESO and 10-O-A. The region between –100°C and 25°C captures thermal transitions relevant to glassy dynamics and polymer segment mobility in asphalt binders.

by a series of perforations and fractures, and shingles treated with SME-O-A and a SESO oil-based emulsion at different concentrations, 10 (10-O-A) and 30 wt% SESO (30-O-A). Old, untreated architectural (U-O-A) shingles bear the brunt of the damage, with numerous points of impact that have compromised the material's structural integrity. These results testify to the vulnerability of aged shingles to the aggressive force of hail. SME-O-A shingles demonstrate comparatively reduced damage, with fewer and smaller visible indentations after the simulated hail impacts. In stark contrast, 10-O-A shingles display remarkable resilience, with fewer and less severe impact marks, suggesting an optimized formulation that fortifies the shingles against such high-energy impacts. However, 30-O-A shingles are overly softened as evidenced by increased damage.

A potential concern in applying oil-based rejuvenating treatments is the possibility of increased flammability. The ASTM E108 Spread of Flame test was conducted to identify any changes in roof flammability related to the treatment. The results are summarized in Figure 10, in which the vertical axis measures the maximum linear extent of fire damage in inches, indicating the material's resistance to flame propagation. Remarkably, the control group, U-O-A, exhibited the *highest* susceptibility to fire, with damage extending nearly to the 50-inch mark. This finding contrasts starkly with the SESO-treated 10-O-A shingles, which significantly curtailed the fire's progression to less than 20 inches, indicating a substantial enhancement in fire-retardant capability. However, 30-O-A shingles showed a nonlinear relationship between treatment concentration and fire resistance, with a slight

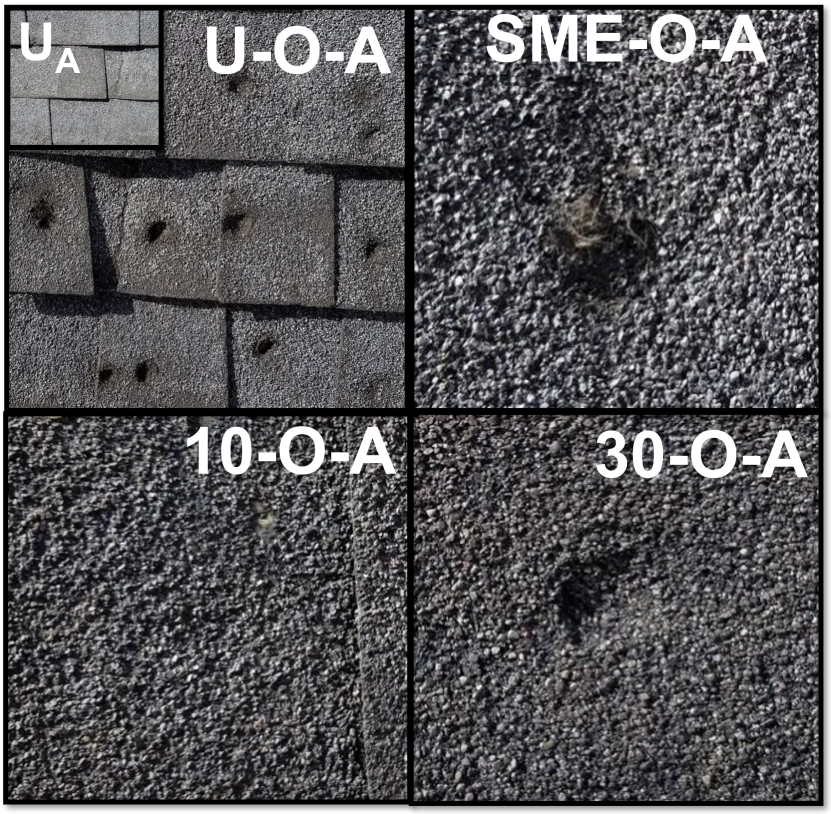


Figure 9 Visual images of asphalt shingles post-impact with different treatments simulating hail damage. The onset image denoted as U_A is an aged, untreated shingle before damage.

rebound in fire spread, although remaining below the extent of damage from the untreated sample. The biodiesel-treated SME-0-A shingles also showed improved fire resistance, but the performance was slightly inferior to the 10-O-A variant.

The improved flame retardancy observed in shingles treated with SESO emulsions, especially at 10 wt%, significantly curtailed flame spread compared to untreated shingles. This finding aligns with the scenario-based fire performance framework outlined by Guillaume [44] and established fire safety engineering principles outlined by Grayson and Hirschler [43], who emphasize that comprehensive fire hazard assessments typically prioritize direct flame spread and heat release tests over simplified ranking metrics, such as oxygen index values. Given this, our utilization of ASTM E108 provides reliable, real-scale flame performance data, strongly indicating that the SESO treatments do not compromise shingle fire safety. Future research, particularly field evaluations, may incorporate oxygen index measurements to complement flame spread data; however, the current evidence sufficiently addresses immediate safety concerns.

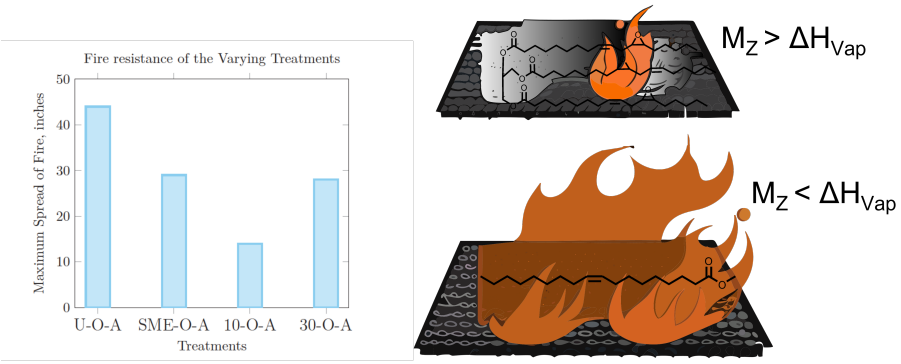


Figure 10 Bar Chart displaying the resistance to the spread of fire

Table S2 provides a detailed overview of key environmental and economic metrics for SESO-based roofing rejuvenation, encapsulating energy consumption and greenhouse gas (GHG) emissions data alongside cost-savings parameters. For instance, the new roof production process is estimated to require approximately 5 kWh/m² of energy and generate around 100 kg CO_2/m² in emissions—figures encompassing material production, processing, and installation. In addition, the table highlights the biogenic carbon credit derived from SESO, where the natural CO_2 uptake during soybean growth contributes an offset of about 480 g CO_2/m², culminating in a net GHG benefit of roughly 2,548 kg CO_2 per 100 m² roof cycle. Moreover, by extending the service life of roofing materials by an estimated 25% (for example, adding five extra years to a 20-year cycle), significant reductions in both energy use and emissions are realized, akin to the reported potential of up to a 33% decrease in energy consumption and a 25% cut in CO_2 emissions for related asphalt technologies. [42, 45, 46]

4. Conclusions

This study investigated the efficacy of SESO emulsions as a rejuvenating agent for asphalt shingles, focusing on their ability to enhance grit adhesion and restore flexibility to aged shingles. In the 3-point bending and granule retention tests, 30 wt% SESO performed the best, followed by 10 wt% SESO and 10 wt% SME. In aged shingles, 10 wt% SESO restored grit adhesion and flexibility closest to that of new shingles, while 30 wt% SESO treatments yielded superior adhesion and flexibility even compared to new shingles. These improvements were also evident in treated new shingles. The exceptional performance of SESO-treated shingles compared to those treated with SME products highlights the potential of SESO emulsions to extend roofing materials' service life and structural performance.

The observed reduction in grit loss is attributed to epoxide rings in SESO, which chemically react with asphaltenes in the asphalt binder to form new covalent bonds. While 30 wt% SESO treatments improved grit retention and flexibility, the associated softening observed in mechanical testing, particularly in flexural modulus, indicates a potential tradeoff in structural rigidity. This finding suggests that overly high SESO loadings may compromise dimensional stability or impact resistance under certain conditions. As such, there is a clear need to optimize SESO content to balance rejuvenation benefits with mechanical performance. Based on the results of this study, SESO concentrations in the range of 10–20 wt% appear to offer a more favorable compromise, restoring key properties without inducing excessive softening. Future studies should refine these limits under varied aging and environmental conditions to define safe and effective application thresholds. These bonds strengthen binder cohesion and aggregate retention, improving mechanical behavior. While the laboratory results are promising, future work should include field validation under natural weathering conditions such as UV exposure, rainfall, and freeze–thaw cycling, to confirm long-term performance and environmental durability.

Acknowledgments

The authors acknowledge the Regents Innovation Fund of the State of Iowa in the support of this work.

Conflicts of Interest

Baker W. Kuehl, Michael Forrester, Nacu Hernandez, Austin Hohmann, R. Chris Williams, and Eric W. Cochran own shares of SoyLei Innovations, LLC. Andrew Becker, Sharan Raman, Anna McCaslin, and Jefferson Roberts-Dobie have no interests to declare.

Declaration of generative AI and AI-assisted technologies in the writing process

During the preparation of this work the author(s) used ChatGPT and Grok in order to compile LCA data summarized from the selected sources. After using this tool/service, the author(s) reviewed and edited the content as needed and take(s) full responsibility for the content of the published article.

References

[1] A. R. M. Association, Asphalt shingles: Raising the b.a.r. (2022).
URL https://www.eia.gov/consumption/manufacturing/data/2014/pdf/Table1_1.pdf

[2] U. E. I. Administration, 2012 commercial buildings energy consumption survey (cbecs) (2015).
URL https://www.eia.gov/consumption/commercial/data/2012/bc/cfm/b1.php

[3] U. E. I. Administration, First use of energy for all purpose (fuel and nonfuel), 2014 (2017).
URL https://www.eia.gov/consumption/manufacturing/data/2014/pdf/Table1_1.pdf

[4] A. R. M. Association, Fourth quarter 2021 report on asphalt roofing product shipments (2021).
URL https://www.asphaltroofing.org/arma-releases-fourth-quarter-2019-report-on-asphalt-roofing-proc

[5] M. Guertin, Roofing with Asphalt Shingles, The Taunton Press, 2002.

[6] T. G. Savvidis, D. Fenistein, L. Barré, E. Béhar, Aggregated structure of flocculated asphaltenes, AIChE Journal 47 (1) (2001) 206–211. doi:10.1002/aic.690470120.
URL https://onlinelibrary.wiley.com/doi/abs/10.1002/aic.690470120

[7] Q. Cui, C. Hurtubise, S. Smith, J. Yang, Asphalt shingle modeling and parameter estimation under short period loading condition, Construction and Building Materials 364 (2023) 129966, description of asphalt shingles' components. doi:10.1016/j.conbuildmat.2022.129966.
URL https://linkinghub.elsevier.com/retrieve/pii/S0950061822036224

[8] A. Brenes-Calderon, A. Vargas-Nordcbeck, Field performance assessment and unsupervised modeling of thin asphalt overlays as preservation treatments for highway pavements, a case study, International Journal of Pavement Research and Technology (2025). doi:10.1007/s42947-025-00504-9.
URL https://doi.org/10.1007/s42947-025-00504-9

[9] N. Darshan, A. V. Kataware, Review on porous asphalt pavements: A comprehensive resolution for stormwater management and applications in current built environment, International Journal of Pavement Research and Technology (2024). doi:10.1007/s42947-024-00444-w.
URL https://doi.org/10.1007/s42947-024-00444-w

[10] M. J. Vámos, J. Szendefy, Temperature effects on traffic load-induced accumulating strains in flexible pavement structures, International Journal of Pavement Research and Technology (2024). doi:10.1007/s42947-024-00466-4.
URL https://doi.org/10.1007/s42947-024-00466-4

[11] A. Arabzadeh, M. D. Staver, J. H. Podolsky, R. C. Williams, A. D. Hohmann, E. W. Cochran, At the frontline for mitigating the undesired effects of recycled asphalt: An alternative bio oil-based modification approach, Construction and Building Materials 310 (2021) 125253. doi:10.1016/j.conbuildmat.2021.125253.
URL https://www.sciencedirect.com/science/article/pii/S0950061821029950

[12] X.-K. Li, G.-S. Chen, M.-W. Duan, W.-C. Yang, S.-C. Tang, Y.-D. Cao, Y. Luo, Branched Hydroxyl Modification of SBS Using Thiol-Ene Reaction and Its Subsequent Application in Modified Asphalt, Industrial & Engineering Chemistry Research 56 (37) (2017) 10354–10365. doi:10.1021/acs.iecr.7b02280.
URL https://doi.org/10.1021/acs.iecr.7b02280

[13] K. Cochran, T. Townsend, Estimating construction and demolition debris generation using a materials flow analysis approach, Waste Management 30 (11) (2010) 2247–2254, statistic regarding shingle waste in landfills every year. doi:10.1016/j.wasman.2010.04.008.
URL https://linkinghub.elsevier.com/retrieve/pii/S0956053X10002175

[14] M. N. Salomé Santos, L. D. Poulikakos, From virgin to recycled bitumen: A microstructural view, Composites Part B: Engineering 80 (2015) 177–185. doi:10.1016/j.compositesb.2015.05.042.
URL https://www.sciencedirect.com/science/article/pii/S135983681500356X

[15] D. M. Mocelin, M. M. Isied, C. Castorena, Influence of reclaimed asphalt pavement (RAP) and recycled asphalt shingle (RAS) binder availability on the composition of asphalt mixtures, Journal of Cleaner Production 426 (2023) 139156, use of RAP and RAS in asphalt mixture compositions. doi:10.1016/j.jclepro.2023.139156.
URL https://linkinghub.elsevier.com/retrieve/pii/S0959652623033140

[16] E. Rinaldini, P. Schuetz, M. N. Partl, G. Tebaldi, L. D. Poulikakos, Investigating the blending of reclaimed asphalt with virgin materials using rheology, electron microscopy and computer tomography, Composites Part B: Engineering 67 (2014) 579–587. doi:10.1016/j.compositesb.2014.07.025.
URL https://www.sciencedirect.com/science/article/pii/S1359836814003059

[17] M. Elkashef, J. Podolsky, R. C. Williams, E. W. Cochran, Introducing a soybean oil-derived material as a potential rejuvenator of asphalt through rheology, mix characterisation and Fourier Transform Infrared analysis, Road Materials and Pavement Design 19 (8) (2018) 1750–1770. doi:10.1080/14680629.2017.1345781.
URL https://doi.org/10.1080/14680629.2017.1345781

[18] X. Shu, B. Huang, D. Vukosavljevic, Laboratory evaluation of fatigue characteristics of recycled asphalt mixture, Construction and Building Materials 22 (7) (2008) 1323–1330. doi:10.1016/j.conbuildmat.2007.04.019.
URL https://www.sciencedirect.com/science/article/pii/S0950061807001225

[19] A. D. Hohmann, M. J. Forrester, M. Staver, B. W. Kuehl, N. Hernández, R. Chris Williams, E. W. Cochran, Chemically mediated asphalt rejuvenation via epoxidized vegetable oil derivatives for sustainable pavements, Fuel 355 (2024) 129374. doi:10.1016/j.fuel.2023.129374.
URL https://www.sciencedirect.com/science/article/pii/S0016236123019889

[20] A. I. Rajib, A. Samieadel, A. Zalghout, K. E. Kaloush, B. K. Sharma, E. H. Fini, Do all rejuvenators improve asphalt performance?, Road Materials and Pavement Design 23 (2) (2022) 358–376. doi:10.1080/14680629.2020.1826348.
URL https://doi.org/10.1080/14680629.2020.1826348

[21] J. H. Podolsky, A. Buss, R. C. Williams, N. Hernández, E. W. Cochran, Effects of aging on rejuvenated vacuum tower bottom rheology through use of black diagrams, and master curves, Fuel 185 (2016) 34–44. doi:10.1016/j.fuel.2016.07.094.
URL http://www.sciencedirect.com/science/article/pii/S0016236116306901

[22] M. Zaumanis, R. B. Mallick, L. Poulikakos, R. Frank, Influence of six rejuvenators on the performance properties of Reclaimed Asphalt Pavement (RAP) binder and 100% recycled asphalt mixtures, Construction and Building Materials 71 (2014) 538–550. doi:10.1016/j.conbuildmat.2014.08.073.
URL https://www.sciencedirect.com/science/article/pii/S0950061814009854

[23] W. Song, B. Huang, X. Shu, Influence of warm-mix asphalt technology and rejuvenator on performance of asphalt mixtures containing 50% reclaimed asphalt pavement, Journal of Cleaner Production 192 (2018) 191–198. doi:10.1016/j.jclepro.2018.04.269.
URL https://www.sciencedirect.com/science/article/pii/S0959652618313118

[24] M. Elkashef, R. C. Williams, E. Cochran, Effect of Asphalt Binder Grade and Source on the Extent of Rheological Changes in Rejuvenated Binders, Journal of Materials in Civil Engineering 30 (12) (2018) 04018319. doi:10.1061/(ASCE)MT.1943-5533.0002526.
URL https://ascelibrary.org/doi/abs/10.1061/%28ASCE%29MT.1943-5533.0002526

[25] R. Zhang, Z. You, H. Wang, M. Ye, Y. K. Yap, C. Si, The impact of bio-oil as rejuvenator for aged asphalt binder, Construction and Building Materials 196 (2019) 134–143. doi:10.1016/j.conbuildmat.2018.10.168.
URL https://www.sciencedirect.com/science/article/pii/S0950061818325789

[26] M. Elkashef, R. C. Williams, E. W. Cochran, Physical and chemical characterization of rejuvenated reclaimed asphalt pavement (RAP) binders using rheology testing and pyrolysis gas chromatography-mass spectrometry, Materials and Structures 51 (1) (2018) 12. doi:10.1617/s11527-018-1141-z.
URL https://doi.org/10.1617/s11527-018-1141-z

[27] M. Elkashef, R. C. Williams, E. Cochran, Investigation of fatigue and thermal cracking behavior of rejuvenated reclaimed asphalt pavement binders and mixtures, International Journal of Fatigue 108 (2018) 90–95. doi:10.1016/j.ijfatigue.2017.11.013.
URL http://www.sciencedirect.com/science/article/pii/S0142112317304395

[28] J. Lin, P. Guo, J. Xie, S. Wu, M. Chen, Effect of Rejuvenator Sealer Materials on the Properties of Aged Asphalt Binder, Journal of Materials in Civil Engineering 25 (7) (2013) 829–835. doi:10.1061/(ASCE)MT.1943-5533.0000702.
URL https://ascelibrary.org/doi/10.1061/%28ASCE%29MT.1943-5533.0000702

[29] Z. Sotoodeh-Nia, N. Manke, R. C. Williams, E. W. Cochran, L. Porot, E. Chailleux, D. L. Presti, A. J. d. B. Carrión, J. Blanc, Effect of two novel bio-based rejuvenators on the performance of 50% RAP mixes – a statistical study on the complex modulus of asphalt binders and asphalt mixtures, Road Materials and Pavement Design 0 (0) (2019) 1–18. doi:10.1080/14680629.2019.1661276.
URL https://doi.org/10.1080/14680629.2019.1661276

[30] R. Romera, A. Santamaría, J. J. Peña, M. E. Muñoz, M. Barral, E. García, V. Jañez, Rheological aspects of the rejuvenation of aged bitumen, Rheologica Acta 45 (4) (2006) 474–478. doi:10.1007/s00397-005-0078-7.
URL https://doi.org/10.1007/s00397-005-0078-7

[31] G. D. Airey, Rheological properties of styrene butadiene styrene polymer modified road bitumens□, Fuel 82 (14) (2003) 1709–1719. doi:10.1016/S0016-2361(03)00146-7.
URL https://www.sciencedirect.com/science/article/pii/S0016236103001467

[32] M. R. Gruber, B. Hofko, Life Cycle Assessment of Greenhouse Gas Emissions from Recycled Asphalt Pavement Production, Sustainability 15 (5) (2023) 4629. doi:10.3390/su15054629.
URL https://www.mdpi.com/2071-1050/15/5/4629

[33] D. Ge, K. Yan, Z. You, H. Xu, Modification mechanism of asphalt binder with waste tire rubber and recycled polyethylene, Construction and Building Materials 126 (2016) 66–76. doi:10.1016/j.conbuildmat.2016.09.014.
URL https://www.sciencedirect.com/science/article/pii/S0950061816314465

[34] S. Miliutenko, A. Björklund, A. Carlsson, Opportunities for environmentally improved asphalt recycling: The example of Sweden, Journal of Cleaner Production 43 (2013) 156–165. doi:10.1016/j.jclepro.2012.12.040.
URL https://www.sciencedirect.com/science/article/pii/S0959652613000024

[35] R. B. Ahmed, K. Hossain, Waste cooking oil as an asphalt rejuvenator: A state-of-the-art review, Construction and Building Materials 230 (2020) 116985. doi:10.1016/j.conbuildmat.2019.116985.
URL https://www.sciencedirect.com/science/article/pii/S0950061819324274

[36] R. Williams, A. Cascione, J. Yu, D. Haugen, M. Marasteanu, J. McGraw, Performance of Recycled Asphalt Shingles in Hot Mix Asphalt, InTrans Project Reports (2013) –.
URL https://lib.dr.iastate.edu/intrans_reports/19

[37] A. A. Cascione, R. C. Williams, J. Yu, Performance testing of asphalt pavements with recycled asphalt shingles from multiple field trials, Construction and Building Materials 101 (2015) 628–642, performance testing of asphalt with RAS in field trials. doi:10.1016/j.conbuildmat.2015.09.027.
URL https://linkinghub.elsevier.com/retrieve/pii/S095006181530386X

[38] C. R. Dixon, F. J. Masters, D. O. Prevatt, K. R. Gurley, Wind Uplift Resistance of Artificially and Naturally Aged Asphalt Shingles, Journal of Architectural Engineering 20 (4) (2014) B4014003, asphalt shingle adherence and unsealing due to weather conditions (wind). doi:10.1061/(ASCE)AE.1943-5568.0000158.
URL https://ascelibrary.org/doi/10.1061/%28ASCE%29AE.1943-5568.0000158

[39] D. Jin, S. Mohammadi, K. Xin, L. Yin, Z. You, Laboratory performance and field demonstration of asphalt overlay with recycled rubber and tire fabric fiber, Construction and Building Materials 438 (2024) 136941. doi:10.1016/j.conbuildmat.2024.136941.

[40] D. Jin, L. Yin, S. Nedrich, K. A. Boateng, Z. You, Resurface of rubber modified asphalt mixture with stress absorbing membrane interlayer: From laboratory to field application, Construction and Building Materials 441 (2024) 137452. doi:10.1016/j.conbuildmat.2024.137452.

[41] D. Jin, K. Xin, L. Yin, S. Mohammadi, B. Cetin, Z. You, Performance of rubber modified asphalt mixture with tire-derived aggregate subgrade, Construction and Building Materials 449 (2024) 138261. doi:10.1016/j.conbuildmat.2024.138261.

[42] P. Boudreaux, S. Pallin, R. Jackson, Investigation of the proposed solar-driven moisture phenomenon in asphalt shingle roofs, Journal of Building Physics (2016) –doi:10.1177/1744259115624183.
URL https://www.osti.gov/biblio/1260070

[43] S. J. Grayson, M. M. Hirschler, Comparison of astm fire standards with international fire standards for buildings and contents, in: A. E. Grand (Ed.), Fire Standards in the International Marketplace, American Society for Testing and Materials, Philadelphia, 1995, pp. 41–60.

[44] E. Guillaume, Fire Analysis Tests from Industrial Point of View, Elsevier, 2022, pp. 381–448. doi:10.1016/B978-0-12-824045-8.00010-1.

[45] F. Ma, A. Sha, R. Lin, Y. Huang, C. Wang, Greenhouse Gas Emissions from Asphalt Pavement Construction: A Case Study in China, International Journal of Environmental Research and Public Health 13 (3) (2016) 351. doi:10.3390/ijerph13030351.

[46] D. M. Barbieri, B. Lou, F. Wang, I. Hoff, S. Wu, J. Li, H. R. Vignisdottir, R. A. Bohne, S. Anastasio, T. Kristensen, Assessment of carbon dioxide emissions during production, construction and use stages of asphalt pavements, Transportation Research Interdisciplinary Perspectives 11 (2021) 100436. doi:10.1016/j.trip.2021.100436.

Restoring Asphalt Shingle Integrity with Soybean Oil-Based Emulsions: A Case Study on Performance, Durability, and Sustainability

Baker W. Kuehl,[‡] Andrew Becker,[‡] Sharan Raman, Anna McCaslin, Jefferson Roberts-Dobie, Michael Forrester, Nacu Hernandez, Austin Hohmann, R. Chris Williams, Eric W. Cochran[a,*]

Electronic Supporting Information

Sample Code	Avg. Flexural Strain (%)	Avg. Max Stress (MPa)	Avg. Flexural Modulus (MPa)
U-N-3T	8.7 ± 0.5	4.3 ± 0.6	7.1 ± 1.6
SME-N-3T	8.6 ± 1.3	4.3 ± 0.2	5.7 ± 0.9
10-N-3T	9.1 ± 1.1	2.5 ± 0.4	4.7 ± 1.4
30-N-3T	8.5 ± 0.9	1.2 ± 0.2	3.0 ± 0.7
U-O-3T	5.9 ± 0.4	7.9 ± 1.0	13.5 ± 3.3
SME-O-3T	7.1 ± 0.6	6.5 ± 0.7	9.1 ± 1.8
10-O-3T	8.7 ± 1.7	4.0 ± 0.2	6.2 ± 1.1
30-O-3T	10.0 ± 1.2	1.9 ± 0.2	2.9 ± 0.4
U-N-A	8.3 ± 0.5	5.5 ± 0.2	12.0 ± 2.4
SME-N-A	7.6 ± 0.5	5.1 ± 0.9	11.0 ± 3.1
10-N-A	9.0 ± 1.1	3.6 ± 0.7	9.1 ± 2.2
30-N-A	9.2 ± 1.0	1.7 ± 0.4	3.3 ± 0.8
U-O-A	7.5 ± 1.6	16.6 ± 1.8	26.2 ± 5.9
SME-O-A	5.9 ± 1.2	5.8 ± 0.9	10.8 ± 2.7
10-O-A	7.0 ± 0.8	4.8 ± 0.7	10.4 ± 1.6
30-O-A	10.5 ± 3.7	2.8 ± 0.4	4.5 ± 1.9

Table S1 The table summarizes the average flexural strain, maximum stress, and flexural modulus for various shingle samples subjected to different treatments. The sample codes denote the type of treatment applied: untreated (U), treated with 10 wt% soybean methyl ester (SME), 10 wt% succinic acid ester of soybean oil (SESO) (10), and 30 wt% SESO (30). The letters N and O signify new and old shingles, respectively, while A and 3T refer to architectural and 3-tab shingles. Each value represents the mean ± standard deviation based on multiple test specimens.

a Department of Chemical & Biological Engineering, Iowa State University, Ames, Iowa 50011, United States .

† Supplementary Information available: Tabulated data, chemical structures. See DOI: 00.0000/00000000.

∗ To whom correspondance should be addressed.

‡ These authors contributed equally to this work.

Table S2 LCA/TCA Metrics for SESO Roofing Applications. The table summarizes key environmental and economic indicators for SESO-based roofing rejuvenation, including application rates, carbon credits, energy consumption, and cost savings.

Parameter	Unit	Value / Calculation	Comments	Sources
SESO Application Rate	mL/m^2	200 mL/m^2	Typical application rate	NA
SESO Density	kg/L	0.92 kg/L	Typical vegetable oil density	[19]
SESO Mass per m^2	kg/m^2	200 mL × 0.92 kg/L = 0.184 kg/m^2	Derived from application rate and density	[19]
Biogenic Carbon Credit	g CO_2/g SESO	2.61 g CO_2/g	CO_2 uptake during soybean growth	[19]
CO_2 Credit per m^2	g CO_2/m^2	0.184 kg/m^2 × 1000 g/kg × 2.61 ≈ 480 g CO_2/m^2	184 g × 2.61 ≈ 480 g CO_2/m^2	[45]
Total CO_2 Credit for 100 m^2 Roof	kg CO_2	480 g/m^2 × 100 m^2 = 48,000 g ≈ 48 kg CO_2	Total biogenic credit over 100 m^2	[45]
New Roof Replacement Emissions	kg CO_2/m^2	100 kg CO_2/m^2	Typical production emissions per m^2	[32]
Extended Service Life Increase	%	25%	Example: 5 extra years on a 20-year cycle	[46]
Avoided CO_2 Emissions (per cycle)	kg CO_2 (100 m^2 roof)	100 m^2 × 100 kg CO_2/m^2 × 0.25 = 2,500 kg CO_2	Savings from extended service life	[46]
Net GWP Benefit (per cycle)	kg CO_2	∼2,548 kg CO_2 (2,500 kg avoided + 48 kg biogenic credit)	Total GHG reduction for 100 m^2	[46]
New Roof Energy Consumption	kWh/m^2	5 kWh/m^2	Energy required per m^2 for production	[32]
Total Energy Consumption for 100 m^2 Roof	kWh	5 kWh/m^2 × 100 m^2 = 500 kWh	Full roof production energy	[32]
Primary Energy Demand	kWh/m^2	∼5 kWh/m^2	For new material production	[45]
Embodied Energy	kWh/m^2 or MJ/m^2	∼5 kWh/m^2	Energy embedded in roofing materials	[19]
Lifecycle Cost Savings (LCCA)	$ (per 100 m^2 cycle)	Assumed 25% cost reduction; e.g., if $100/$m^2$, saving = $2,500	Based on reduced replacement frequency	[19]
Payback Period / NPV Impact	Years / $	Improved NPV due to fewer replacements (e.g., payback in 5–10 years)	Depends on initial treatment cost vs. savings	[19]
Additional Environmental Impacts	Various impact units	Reduced acidification, eutrophication, toxicity impacts	Indirect benefits from reduced production demand	[19], [45]
Resource & Waste Savings	% or tons saved	∼25% reduction in material consumption and waste per cycle	Due to extended roof life	[19]

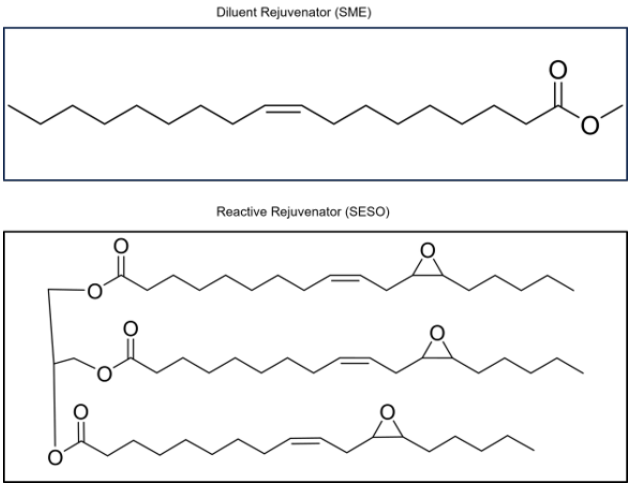


Figure S1 The top image illustrates the molecular structure of soybean methyl ester (SME), a monomeric compound used for treating shingles. The bottom image shows the chemical structure of sub-epoxidized soybean oil, which includes partially epoxidized chains derived from soybean oil.

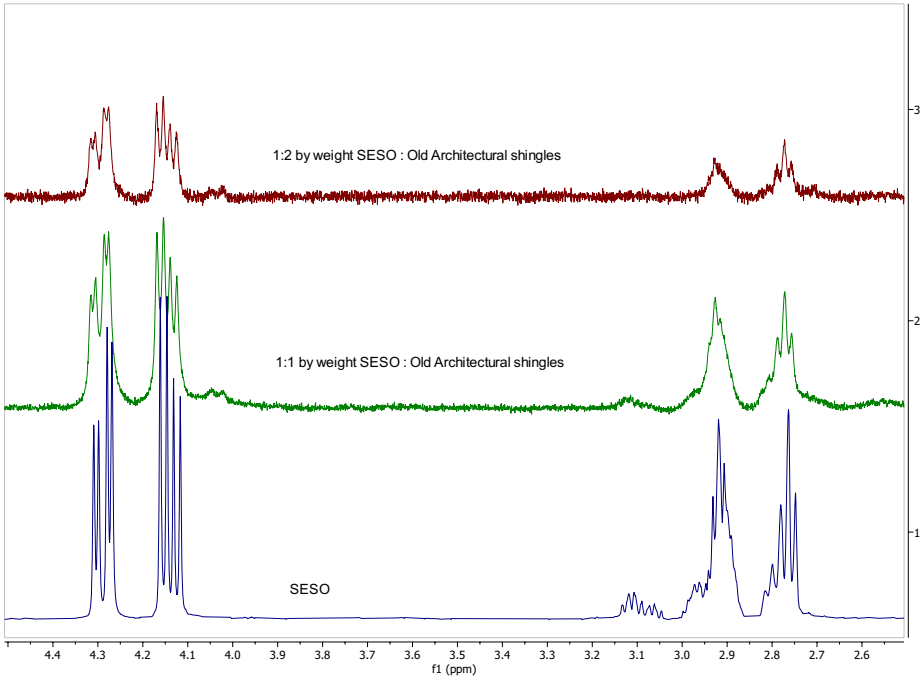


Figure S2 1H NMR spectra demonstrating the reactivity of SESO with asphalt from aged shingles. Vials containing pure SESO, a 1:1 weight ratio of SESO to crumbled shingles, and a 1:2 ratio were stirred at 180°C for 5 hours. The oxirane proton signal between 2.7–3.3 ppm progressively diminished with increasing shingle content, indicating consumption of epoxide groups. Integration of these peaks relative to SESO's backbone protons revealed that the oxirane-to-SESO ratio decreased from 2.34 in the pure material to 1.18 in the 1:1 mixture and to 0.92 in the 1:2 mixture.